JOURNAL OF GUIDANCE, CONTROL, AND DYNAMICS
Vol. 19, No. 3, May–June 1996

Synchronization of Twin-Gyro Precession Under Cross-Coupled Adaptive Feedforward Control

Li-Farn Yang* and Wen-Hua Chang†
National Chung Cheng University, Taiwan, Republic of China

Cross-coupled adaptive feedforward control represents an emerging approach to synchronizing the precession of twin gyros of control-moment-gyro (CMG) devices intended for use in the slewing maneuvers of space structures. The gyro control system features the integration of an adaptive controller and a feedforward controller for each gyro control axis. Then, two such control mechanisms are linked together by a coupling law, in which an error in either gyro axis can affect overall control loops so that the disturbed axis is rapidly recovered with the undisturbed axis for the synchronous precession. This adaptive synchronization problem is formulated and analyzed along with a twin-gyro CMG model, and the adaptation law is optimally designed through an optimization process in an attempt to minimize the synchronization errors from twin-gyro precession. Simulated-time histories of CMG-driven slewing maneuvers under the synchronization control are presented to show the effectiveness of the present approach.

I. Introduction

MANEUVERABLE space structures, which undergo slewing motions for either targeting or station-keeping tasks, have received increasing attention in recent years. Studies[1–8] performed so far indicate that the control-moment-gyro (CMG) devices have been used very effectively for attitude control of spacecrafts essentially because of their large momentum-exchange capacity. For instance, single-gimbaled CMGs have been installed on the MIR Space Station, whereas double-gimbaled CMGs were used in NASA Skylab and are proposed for use on Space Station Freedom.[1] On the other hand, CMGs can be used as a way to augment structural damping for vibration suppression purposes. In doing so, NASA's Mini-Mast Facility[2] has adopted a torque wheel as an active damper, and Montgomery et al.[3] employed a hub actuator along with a torque wheel in a complementary way to suppress the flexural vibration of a slewing arm. In the experiments of Refs. 2 and 3, CMGs are viewed as energy sinks in the system to dissipate mechanical energy, and they become very effective over a broad range of frequencies, whereas a passive damper is generally effectively tuned for a narrow frequency range.

The CMG dynamics are inherently nonlinear as the result of the nonlinearities in gimbal geometry, coupling orientation, and momentum saturation (or singularity) among the various gyro axes. These nonlinear characteristics require an increase in the modeling complexity, estimation, and control of CMG devices. Also, the performance of CMGs is very sensitive to the unpredictable disturbances that can give rise to poor momentum management among gyro control axes, and thereby resulting in momentum singularity and even in instability of the gyro control system. Various steering laws have been studied for active control of CMGs, such as feedback linearization control,[1] momentum desaturation control,[5] and roll/yaw coupling control.[8] These papers were aimed at using the respective approach to manage CMG momentum so as to output a desired torque for executing attitude control of spacecrafts.

Recently, Yang et al.[4] proposed a feedforward/feedback moment-gyro control for an effective use of CMGs in concurrent maneuvering and vibration suppression on space structures, and applied this concept to a flexible truss arm with onboard CMGs subjected to single-axis motions. Figure 1 shows a perspective of this CMG-equipped system, which can be applied as a transportation means for astronauts or components during in-space construction. The CMG device consists of a pair of twin gyros that must synchronously precess for proper momentum exchange with the slewing structures. For a multigyro (or multigimbaled) CMG device, the effects of poor synchronization between two gyro control axes are all adverse and result in unbalance of gyrotorquing and even in momentum saturation. The objective of this paper is thus to conduct the synchronous precession of twin-gyro CMGs from the standpoint of adaptive control: in particular, concurrent position and speed synchronization of two gyro motions under an integrated cross-coupled, adaptive, and feedforward control[9] is considered.

In this paper, an adaptive control scheme is proposed to achieve the motion synchronization for a twin-gyro system so as to coordinate two gyro motions against disturbances that may degrade CMG momentum management for gyrotorquing space structures. The adaptive synchronization system consists of an adaptive controller and a feedforward controller for each gyro control axis. Then, two such gyro controllers are linked together by a coupling law, which is introduced in response to a synchronization error, i.e., the difference between two motion errors of twin gyros, as a compromise for the synchronization control. In this way, an error in either gyro axis can affect overall control loops so that a disturbed axis is recovered with another undisturbed axis in a complementary way. The stability of the overall control system is also analyzed to quantify the stability margin of the controller for CMG-driven slewing maneuvers of space structures.

The outline of the remainder of this paper follows. First, the description of the system is presented followed by the derivation of equations of motion for a truss-arm system incorporating a CMG device. Then, the cross-coupled adaptive feedforward control is developed and applied to the CMG synchronization problem, followed by an optimization procedure for the control system. Finally, control simulation results are presented for discussion.

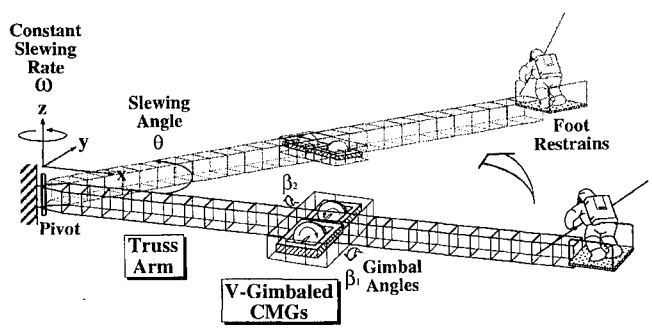

Fig. 1 Slewing truss with twin-gyro CMGs.

Received Oct. 3, 1994; revision received Jan. 17, 1996; accepted for publication Jan. 24, 1996.

*Associate Professor, Department of Mechanical Engineering. AIAA Member.

†Research Assistant, Department of Mechanical Engineering.

II. Dynamics of a CMG-Truss System

In this section, dynamics of a truss arm and CMGs are studied and incorporated into a CMG-equipped system, as shown in Fig. 1. Figure 2 shows the configuration of the CMGs, which are composed of a pair of identical, coaxially gimbaled gyros that can be driven to precess about the gimbal axes by two motors. In Fig. 2, three conditions of CMGs are illustrated for discussion: 1) in nominal status, two gyros face to each other so that the counter-rotation of two spinning rotors cancels the internally stored momenta; 2) in synchronous status, two gyros precess in a synchronous fashion such that the resultant gyro momentum always remains aligned with the momentum exchange axis; and 3) in asynchronous status, two gyros precess out of synchronization in the presence of disturbances, which in turn triggers unbalanced coupling momenta; thereby, the momentum management of the gyro system cannot hold.

The truss-arm system as shown in Fig. 1, if properly installed with the CMGs onboard, is then capable of undergoing slewing motions under CMG actuation. Assume that the angular displacement and velocity of the truss arm are introduced as θ and $\dot{\theta}$, respectively, whereas the gimbal angles and their time-derivative counterparts are indicated by β_i and $\dot{\beta}_i$, respectively. For the system as presented in Fig. 1, the total energy can be expressed by

$$2T = I\dot{\theta}^2 + \sum_{i=1}^{2} J\left(\dot{\theta}^2 + \dot{\beta}_i^2\right) \tag{1}$$

where I is the effective moment of inertia of the system and J is the moment of inertia of the CMG rotor. Applying the principle of virtual work, one may express the virtual work done by the applied inputs as

$$\delta W = \sum_{i=1}^{2} [u_i \delta\beta_i + h_{\text{cmg}} \cos(\beta_i)\dot{\beta}_i \delta\theta] \tag{2}$$

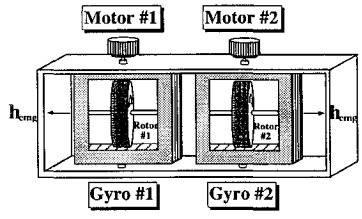

a) Nominal status

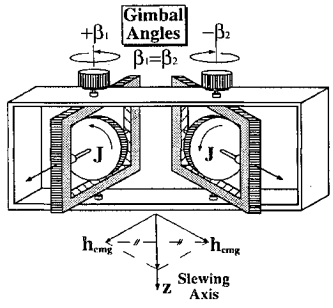

b) Working status

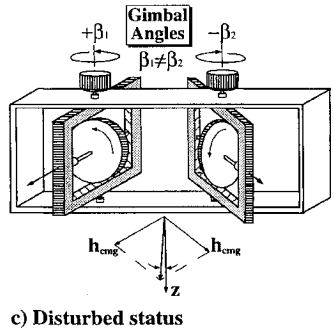

c) Disturbed status

Fig. 2 Configuration of twin-gyro CMGs.

where u_i denotes the control inputs about the gyro axes of the CMGs and h_{cmg} indicates the constant angular momentum stored in the gyros. Via Lagrange's method, the equations of motion of such a CMG-equipped system can be derived by using Eqs. (1) and (2) and written in the following matrix form:

$$\begin{bmatrix} I & 0 & 0 \\ 0 & J & 0 \\ 0 & 0 & J \end{bmatrix} \begin{bmatrix} \ddot{\theta} \\ \ddot{\beta}_1 \\ \ddot{\beta}_2 \end{bmatrix} = h_{\text{cmg}} \begin{bmatrix} 0 & -\cos(\beta_1) & -\cos(\beta_2) \\ \cos(\beta_1) & 0 & 0 \\ \cos(\beta_2) & 0 & 0 \end{bmatrix} \times \begin{bmatrix} \dot{\theta} \\ \dot{\beta}_1 \\ \dot{\beta}_2 \end{bmatrix} + \begin{bmatrix} 0 \\ u_1 \\ u_2 \end{bmatrix} + \begin{bmatrix} 0 \\ d_1 \\ d_2 \end{bmatrix} \tag{3}$$

Observe that the first term of the right-hand side is the gyroscopic damping matrix, the second is the input vector, and the last includes two disturbances, i.e., d_1 and d_2, to the gimbal pair. Now, if gyros 1 and 2 are synchronized during precessing, we can equate $\beta_2 \approx \beta_1$ and $\dot{\beta}_2 \approx \dot{\beta}_1$ in Eq. (3) and obtain

$$I\dot{\theta} = -2h_{\text{cmg}} \sin(\beta_1) \tag{4}$$

$$2J\ddot{\beta}_1 + \frac{2h_{\text{cmg}}^2}{I} \sin(2\beta_1) = u_1 \tag{5}$$

Equation (4) shows the concept of momentum exchange, viz., if the slewing momentum of the truss arm increases, then the CMGs lose an equal amount of gyro momentum. It can also be seen that Eq. (5) illustrates a forced vibration problem, in which the gyros will wobble back and forth in a synchronous manner at the frequency $f = (h_{\text{cmg}}/2\pi)\sqrt{(2/IJ)}$, provided that the gimbal angle is small. This phenomenon is akin to a pendulum vibration problem in the gravitational field.

Now, an attempt will be made to design the synchronization control system in terms of an adaptive feedforward control scheme for the CMGs atop a truss-arm system, which will be presented in the following section.

III. Synchronization Control Design

As alluded to earlier, a special control concept must be introduced to CMGs incorporating the slewing control for space structures. In this paper, we present a concept that makes concurrent use of adaptive control as well as feedforward control, and assesses its applicability to synchronization control on CMGs. In so doing, the time-varying output signals from CMGs are regulated and tracked on the prescribed trajectories in such a way as to synchronize the twin gyros during precessing. Figure 3 shows a control block diagram of the proposed gyro control system, which is composed of 1) a reference model, 2) a pair of feedback controllers, 3) a pair of adaptive feedforward controllers, and 4) two coupling gains.

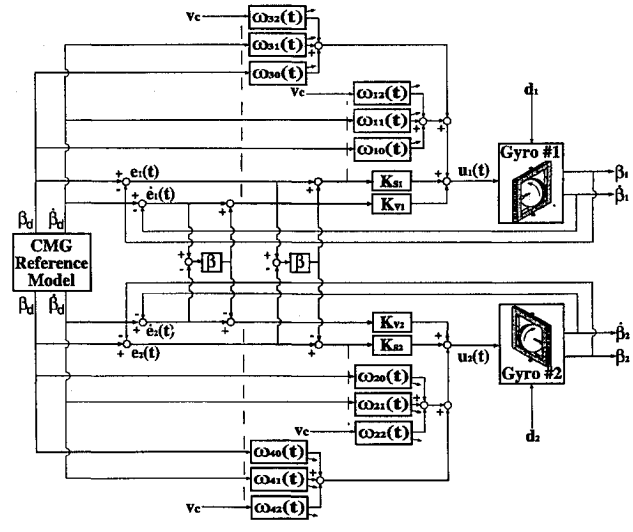

Fig. 3 Synchronization control block diagram for twin-gyro system.

As demonstrated in Fig. 3, the adaptive control pair is model based, which requires a reference model as guideline for tracking control. A reference model is set up in the loop and triggered by a designated input u_0, to provide the time-history trajectories of gimbal angle β_d and gimbal velocity $\dot{\beta}_d$, as desired. Then, corresponding to the disturbed dynamic responses, the errors $e_i(t)$ and $\dot{e}_i(t)$ can be obtained by $e_i(t) = \beta_d - \beta_i$ and $\dot{e}_i(t) = \dot{\beta}_d - \dot{\beta}_i$, respectively. These errors are regulated through a pair of feedback controllers characterized by a constant control law $[k_{si}\ k_{vi}]$ incorporating a variant adaptation law $[\omega_{sij}\ \omega_{vij}]$ for the compensation of the tracking errors in response to the disturbances. Finally, a coupling parameter α is introduced to compromise two differential errors such as $\epsilon(t) = e_1(t) - e_2(t)$ and $\dot{\epsilon}(t) = \dot{e}_1(t) - \dot{e}_2(t)$ in a complementary way to achieve a concurrent position/speed synchronization as is demanded in this paper. A complete derivation of this control synthesis is presented in the following subsections.

A. Reference Model

A feedforward input to CMGs has been selected from Ref. 4 as a driving force to trigger a desired slewing motion of the truss arm for the investigation of the twin-gyro synchronization problem. Such a gyro input was derived in closed form directly from Eqs. (4) and (5) under the assumption that the two gyros be perfectly synchronized in the precession, and it is expressed as

$$u_0 = -\frac{I\omega^2}{2\sin^{-1}(I\omega/2h_{\text{cmg}})}\left[1 - \left(\frac{I\omega}{2h_{\text{cmg}}}\right)^2\right] \tag{6}$$

where ω denotes the mean velocity of the slewing rate, viz., $\dot{\theta}$, as assigned by an autopilot prior to maneuvers. Subjected to the input u_0, the gimbals will shift to an offset angle (β_{offset}) while wobbling around it at the frequency $f_w = (h_{\text{cmg}}/2\pi)\sqrt{(2/IJ)}$, and the truss will slew like a constant-rate motion with small oscillations superimposed on it. The angle β_{offset} can be explicitly expressed by

$$\beta_{\text{offset}} = -\frac{1}{2}\sin^{-1}\frac{I\omega}{2h_{\text{cmg}}} \tag{7}$$

In Eq. (6), the feedforward input is characterized by a closed-form function of a dimensionless parameter $I\omega/2h_{\text{cmg}}$, which is a ratio of momentum exchange of the slewing momentum to that stored in the CMGs. Such a ratio must be bounded by $|I\omega/2h_{\text{cmg}}| \le 1$, implying that the desired slewing momentum cannot exceed the stored gyro momentum to avoid CMG momentum saturation that may degrade the CMG performance. In this way, the magnitude of the feedforward input u_0 can be predetermined if the slewing rate ω is a given.

A reference model of the synchronous gyros is then formed by Eqs. (4–6) to generate the desired trajectories of β_d and $\dot{\beta}_d$ as needed for the proposed control loop in Fig. 3. A simulation of 30-deg slew in 50 s is implemented using the proposed input u_0 in Eq. (6) for the model with parameters shown in Table 1. Figure 4 shows the time-history responses of the slew angle and gimbal angles with/without a 10-deg offset applied to the second gimbal axis at the initial time. It can be seen that the two gimbals, if offset initially, drift out of synchronization so that their momentum axes are misaligned, and thereby the slewing system becomes unstable.

The simulation results in Fig. 4 indicate that an asynchronous motion of two gyros caused by a disturbance poses a severe restriction on the CMG operation for slewing maneuvers of a truss-arm system. In the next two subsections, we propose a cross-coupled adaptive feedforward control approach to deal with this problem.

Table 1 Model parameters of a CMG-truss system

Truss arm	
Moment-of-inertia, lbf-in.^{2}	$I = 59690.0$
CMG device (Bendix Model MA-500AC)	
Moment-of-inertia, lbf-in.^{2}	$J_1 = 25.0$
Moment-of-inertia, lbf-in.^{2}	$J_2 = 25.0$
Gyro momentum, lbf-in.-s	$h_{\text{cmg}} = 6126.0$
Limit angle, deg	$\beta_a = 45$
Feedback control law	
Control gain	$k_{s1} = k_{s2} = 5$
Control gain	$k_{v1} = k_{v2} = 1$

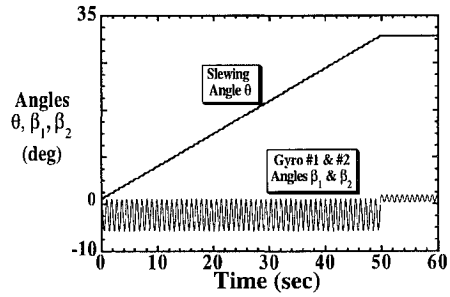

a) Synchronous motion

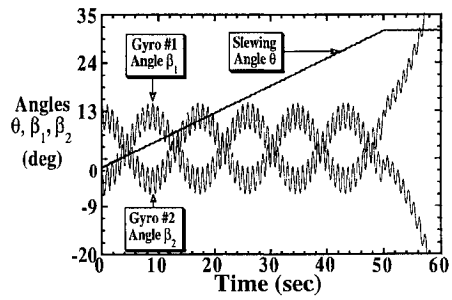

b) Asynchronous motion

Fig. 4 Dynamic responses of asynchronous gyro precession.

B. Adaptive Feedforward Control

Feedforward control is known to be very effective in tracking the time-varying desired output signal as long as the plant model is accurate. Adding adaptation into the feedforward control can enable the entire system to deal with varying plant parameters and to eliminate the steady-state error caused by the feedforward controller in each gyro axis. To design the adaptive feedforward control, we start with the control inputs to the gyro system. As shown in Fig. 3, the two inputs to gyros 1 and 2 can be expressed by the following matrix equation:

$$u_i(t) = k_{si}e_i(t) + k_{vi}\dot{e}_i(t) + u_{fi}(t), \qquad i = 1, 2 \tag{8}$$

which contains a linear regulator and an adaptive controller. The errors $e_i(t)$ vary as a result of the differences between β_d and β_i when either of the twin gyros deviate from the synchronous trajectory. In Eq. (8), the last term can be tuned through the adaptation law in a way that

$$u_{fi}(t) = [\omega_{si0}(t) + \omega_{vi0}(t)]\beta_d + [\omega_{si1}(t) + \omega_{vi1}(t)]\dot{\beta}_d + [\omega_{si2}(t) + \omega_{vi2}(t)]v_c, \qquad i = 1, 2 \tag{9}$$

Equation (9) accounts for the compensation of two desired signals β_d and $\dot{\beta}_d$ from the preceding reference model, and v_c is a constant that is used for canceling the disturbances d_1 and d_2 in adaptation. The value of v_c is chosen so that $\|v_c\| \sim \|\beta_d\|$ (Ref. 9). Moreover, the time variant $\omega_{sij}(t)$ and $\omega_{vij}(t)$ can be tuned separately for $u_{fi}(t)$ by

$$\begin{gathered}\dot{\omega}_{si0}(t) + \omega_{si0}(t) = \gamma\beta_d e_i(t) \\ \dot{\omega}_{vi0}(t) + \omega_{vi0}(t) = \gamma\beta_d\dot{e}_i(t), \qquad \dot{\omega}_{si1}(t) + \omega_{si1}(t) = \gamma\dot{\beta}_d e_i(t) \\ \dot{\omega}_{vi1}(t) + \omega_{vi1}(t) = \gamma\dot{\beta}_d\dot{e}_i(t), \qquad i = 1, 2 \\ \dot{\omega}_{si2}(t) + \omega_{si2}(t) = \gamma v_c e_i(t), \qquad \dot{\omega}_{vi2}(t) + \omega_{vi2}(t) = \gamma v_c\dot{e}_i(t)\end{gathered} \tag{10}$$

where γ is a positive adaptation gain for both adjusting mechanisms. Notice that $\omega_{sij}(t)$ with the subscript s are driven by the position

error $e_i(t)$ in those first-order differential equations, whereas $\omega_{vij}(t)$ with the subscript v are influenced by the rate error $\dot{e}_i(t)$. Thereby, simultaneous synchronization of position and rate in the gyroscopic precession is made feasible.

C. Coupling Control

For better position/speed synchronization between gyros 1 and 2, one can measure two differential errors such that

$$\epsilon(t) = e_1(t) - e_2(t) \qquad \text{and} \qquad \dot{\epsilon}(t) = \dot{e}_1(t) - \dot{e}_2(t) \tag{11}$$

Then, those two adaptive mechanisms in the previous subsection can be cross-linked by means of a coupling parameter α, and Eq. (10) can be rewritten to be

$$\dot{\hat{\omega}}(t) + \hat{\omega}(t) = \gamma\Phi(t)[\hat{e}(t) + \alpha E\hat{\epsilon}(t)] \tag{12}$$

where the vectors $\hat{\omega}(t)$, $\hat{e}(t)$, and $\epsilon(t)$, and the matrices $\Phi(t)$ and E become

$$\hat{\omega}(t) = [\omega_{s10}(t)\omega_{s11}(t)\omega_{s12}(t)\omega_{s20}(t)\omega_{s21}(t)\omega_{s22}(t)\omega_{v10}(t)\omega_{v11}(t)\omega_{v12}(t)\omega_{v20}(t)\omega_{v21}(t)\omega_{v22}(t)]^T$$

$$\hat{e}(t) = [e_1(t) \quad e_2(t) \quad \dot{e}_1(t) \quad \dot{e}_2(t)]^T$$

$$\hat{\epsilon}(t) = [\epsilon(t) \quad \dot{\epsilon}(t)]^T$$

$$\Phi(t) = \begin{bmatrix} \beta_d(t) & 0 & 0 & 0 \\ \dot{\beta}_d(t) & 0 & 0 & 0 \\ v_c & 0 & 0 & 0 \\ 0 & \beta_d(t) & 0 & 0 \\ 0 & \dot{\beta}_d(t) & 0 & 0 \\ 0 & v_c & 0 & 0 \\ 0 & 0 & \beta_d(t) & 0 \\ 0 & 0 & \dot{\beta}_d(t) & 0 \\ 0 & 0 & v_c & 0 \\ 0 & 0 & 0 & \beta_d(t) \\ 0 & 0 & 0 & \dot{\beta}_d(t) \\ 0 & 0 & 0 & v_c \end{bmatrix} \tag{13}$$

$$\text{and} \qquad E = \begin{bmatrix} 1 & 0 \\ -1 & 0 \\ 0 & 1 \\ 0 & -1 \end{bmatrix}$$

Notice that, in Eq. (12), the differential equations of those adaptation variables are driven by the synchronization errors in addition to the tracking errors. The coupling parameter α in Eq. (12) must be chosen to be positive so that the state matrix in Eq. (A1) (see the Appendix) carries stable eigenvalues to guarantee the asymptotic stability of the overall system. Equation (12) thus provides a set of cross-coupled differential equations capable of adjusting the adaptation law in cooperation with the feedback control toward an integrated synchronization control for a CMG system adaptive to the changing environment. Also, note that the synchronization errors drive these two sets of adaptation algorithms in opposite directions, which results in faster removal of the synchronization errors. The overall adaptive system is stable provided that α and γ are positive to ensure the positive definiteness of Eq. (A1) (see the Appendix) and that the desired output and its derivative β_d and $\dot{\beta}_d$ are bounded.

Thus, cross-coupled, adaptive, and feedforward control synthesis is accomplished for synchronization control of a twin-gyro CMG system. Now, an attempt should be made to arrange an optimization problem in search of a set of optimum control parameters for the minimization of the synchronization errors. This will be the subject of the next section.

IV. Optimization of Control System

In this section, a control optimization is presented to find the optimum solution of the control parameters α and γ, as given in Eq. (12), to minimize the synchronization errors specified by Eq. (11). The optimization problem is formulated to minimize the integral of mean-squared value of the tracking errors so that the optimization problem is expressed as follows.

Minimize:

$$F(\boldsymbol{y}) = \int_0^{t_f} t\hat{e}(t)^T\hat{e}(t)\,dt = \sum_{i=1}^{n} t_i\hat{e}(t_i)^T\hat{e}(t_i)\Delta t$$

$$\hat{e}(t_i) = [e_1(t_i)\ e_2(t_i)\dot{e}_1(t_i)\ \dot{e}_2(t_i)]^T \tag{14}$$

Subject to:

$$\phi(\boldsymbol{y}) = \dot{\hat{\omega}}(t) + \hat{\omega}(t) - \gamma\Phi(t)[\hat{e}(t) + \alpha E\hat{\epsilon}(t)] = 0 \tag{15}$$

where

$\boldsymbol{y}$ = vector of design variables, $[\alpha\ \gamma]^T > 0$
$F(\boldsymbol{y})$ = cost function of design variable vector $\boldsymbol{y}$
$\phi(\boldsymbol{y})$ = equality constraint function

In Eqs. (14) and (15), the optimization program uses the polytope algorithm[10] to seek the optimum solution of the design variables to minimize a cost function $F(\boldsymbol{y})$. The lower bounds are imposed on the positive design variables. As demonstrated in the Appendix, the positiveness of the design variables can avoid the instability of the adaptive system for each new search point during the optimization process. Following the procedure of optimization, the cross-coupled adaptation algorithm given by Eq. (15) is numerically integrated in time for the simulation of the equations of motion (3) triggered by a specified disturbance to obtain the time-history responses that are discretely sorted at an even interval for the determination of the cost function defined in Eq. (14). Therefore, Eq. (15) serves as an equality constraint imposed upon this optimization problem. Above all, minimization of this cost function is also subject to optimization with respect to t_f so that the resulting errors will be quickly diminishing.

Based on Eqs. (14) and (15), the optimization of the CMG control system is carried out by implementing a 45-deg slew maneuver in 10 s along with an impulsive disturbance −0.5 lbf-in. imposed on gyro 1. The discrete parameters in Eq. (14) are assigned the values $n = 1000$ and $\Delta t = 0.01$ s, respectively. The feasible starting point is specified to be $\boldsymbol{y} = [18\ \ 25]^T$. At this starting point, the value of the cost function $F(\boldsymbol{y})$ equals 4.65×10^7, whereas the final cost is 3.22×10^6 at the minimum of $F(\boldsymbol{y})$. By using the polytope algorithm with the design parameters given in Table 1, the solution to this optimization problem has been found to be: $\boldsymbol{y}_{\text{opt}} = [\alpha_{\text{opt}}\ \gamma_{\text{opt}}]^T = [11\ \ 48]^T$. Although not described herein, the optimum result given here is shown to be insensitive to disturbances.

V. Numerical Results

The model parameters of the CMG-truss system for the simulations are summarized in Table 1. Two kinds of synchronization controls have been employed for simulation: one is with regular adaptation parameters given by $[\alpha\ \gamma] = [18\ 25]$ and another is with the optimum design ($[\alpha_{\text{opt}}\ \gamma_{\text{opt}}] = [11\ 48]$) from Sec. IV. A 45-deg slew task in 10 s is assigned to the CMG-truss system undergoing forward-and-backward slewing maneuvers with a 10-s intermission in between. The simulations are implemented for the slewing maneuvers of the CMG-truss system subjected to a sequence of impulsive disturbances on gyro 1. In so doing, the feedforward torque alternates between $u_0 = \pm 800.0$ lbf-in. in three steps, the offset angle of gimbals $\beta_{\text{offset}} = -22.5$ deg, and the wobble frequency $f_w = 2.1$ Hz.

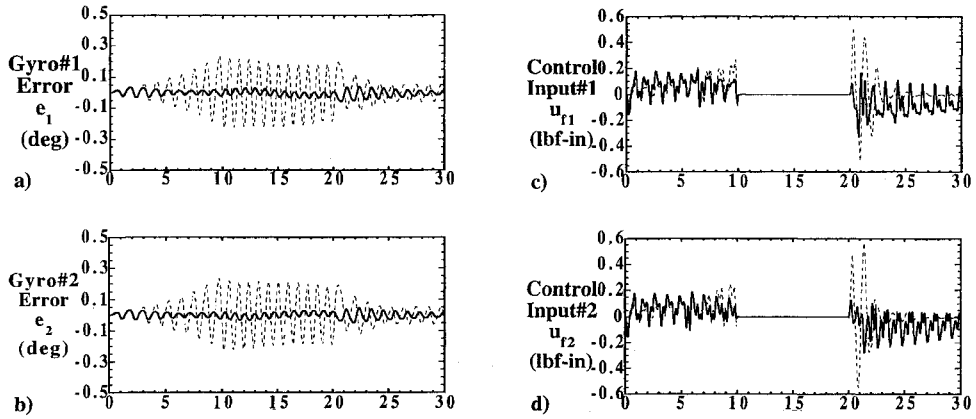

Fig. 5 Simulation results of slewing maneuvers of a CMG-truss arm subjected to impulsive disturbances.

Figure 5 shows the 30-s numerical results of twin-gyro control simulations disturbed by three distinct impulses upon gyro 1. The three impulses are 0.5, 0.2, and 0.2 lbf-in. in magnitude acting on the axes x_1, x_2, and y_1 at 5.4, 12.4, and 22.4 s, respectively. The truss arm travels to the 45-deg destination in 10 s, rests for 10 s in that position, and returns to the original position with the same speed. The results associated with the optimal synchronization control and its regular counterpart are indicated by a solid line and a dotted line, respectively. Since the synchronous precession has been accomplished on twin gyros here, the time histories of the slewing angle and the gyro angles for these two kinds of controllers are consistent with those that have been shown by Fig. 3a and also have been discussed in Sec. III. Figures 5a and 5b show the responses of the tracking errors of gyros 1 and 2, respectively. It can be seen that the errors of two gyros are synchronized during the twin-gyro precession and are strictly restrained within the range of ±0.3 deg. Moreover, the errors on the solid lines are considerably suppressed as compared to those on the dotted lines because of the optimality embedded in the solid lines. The responses of two adaptive control inputs responding to the tracking errors are shown in Figs. 5c and 5d, respectively.

To achieve better synchronization, we used an optimization problem formulated to work for the optimality of an adaptive control system, wherein the control parameters were optimally determined under the stability criteria. The cross-coupled adaptive feedforward control as designed and integrated through the optimization process have been shown to be applicable and suitable for the synchronization control of CMGs in gyrotorquing the slewing space structures.

Simulation results have demonstrated the effectiveness of the proposed approach in motion synchronization for the CMGs subjected to the input disturbances. However, much work needs to be done before applying the proposed strategy to real spacecraft. The issues that should be investigated include the robustness, cost effectiveness, and weight penalty.

Appendix: Stability Analysis of Gyro Control System

If the feedback representation in Fig. 3 is formed by the error signal in the state space, it can be readily recognized that the following equation is satisfied for the adaptive synchronization control system:

$$\begin{bmatrix} \dot{e}_1 \\ \dot{e}_2 \\ \ddot{e}_1 \\ \ddot{e}_2 \end{bmatrix} = \begin{bmatrix} 0 & 0 & 1 & 0 \\ 0 & 0 & 0 & 1 \\ -\dfrac{\left[\left(h_{\text{cmg}}^2/I\right)+k_{s1}(1+\alpha)\right]}{J} & -\dfrac{\left(h_{\text{cmg}}^2/I\right)-k_{s1}\alpha}{J} & -\dfrac{k_{v1}(1+\alpha)}{J} & -\dfrac{k_{v1}\alpha}{J} \\ -\dfrac{\left(h_{\text{cmg}}^2/I\right)-k_{s2}\alpha}{J} & -\dfrac{\left[\left(h_{\text{cmg}}^2/I\right)+k_{s2}(1+\alpha)\right]}{J} & \dfrac{k_{v2}\alpha}{J} & \dfrac{k_{v2}(1+\alpha)}{J} \end{bmatrix} \begin{bmatrix} e_1 \\ e_2 \\ \dot{e}_1 \\ \dot{e}_2 \end{bmatrix} \tag{A1}$$

The two gyro motions have been shown to be synchronized in tracing a desired trajectory so that the errors in the tracking control are effectively suppressed in a complementary way. The simulation results thus validate the potential applicability of the proposed gyro control design for CMG-driven slewing structures.

VI. Concluding Remarks

The problem of synchronization for twin-gyro precession of CMGs has been proposed and analyzed under cross-coupled adaptive feedforward control. The basic idea of the proposed strategy is to synchronously steer a pair of precessing gyros for momentum exchange with space structures, while attempting to maneuver the slewing structures under the CMG actuation. An adaptive feedforward controller has been developed for each gyro control axis, and then two such controllers were cross coupled using the coupling law so that these two gyro controllers can compromise the differential errors for motion synchronization. The stability of the control system was also analyzed to set criteria for the control parameters.

If we assume $k_{s1} = k_{s2} = k_s$ and $k_{v1} = k_{v2} = k_v$ in Eq. (A1), the eigenvalues of the state matrix can be derived in closed form such that

$$\lambda_{1,2} = -\frac{k_v}{2} \pm j\sqrt{\frac{2h_{\text{cmg}}^2}{I} + k_s - \left(\frac{k_v}{2}\right)^2} \tag{A2}$$

$$\lambda_{3,4} = -\frac{(1+2\alpha)k_v}{2} \pm j\sqrt{(1+2\alpha)k_s - \left[\frac{(1+2\alpha)k_v}{2}\right]^2} \tag{A3}$$

which indicates that such a control system is asymptotically stable if and only if the real parts of λ_i are negative, implying $k_v > 0$ and $\alpha > -\frac{1}{2}$. Since the α is to deal with the difference of errors $e_1(t)$ and $e_2(t)$ as defined in Eq. (11), it is usually chosen to be positive, i.e., $\alpha > 0$. If the imaginary part of $\lambda_{3,4}$ is positive, one can obtain $k_s > [(1+2\alpha)/4]k_v^2 > 0$. If it is negative, the $\lambda_{3,4}$ become two negative real eigenvalues. Therefore, the control parameters α, k_s, and k_v are positive in the sense of asymptotic stability.

Acknowledgment

The authors wish to acknowledge the support of this investigation through NSC Grant 84-2212-E-194-011 from the National Science Council in Taiwan.

References

[1]Dzielski, J., Rowell, D., and Wormley, D., "Approach to Control Moment Gyroscope Steering Using Feedback Linearization," *Journal of Guidance, Control, and Dynamics*, Vol. 14, No. 1, 1991, pp. 96–106.

[2]Tanner, S., Ghosh, D., and Kenny, S., "Mini-Mast CSI Test Bed Users Guide," NASA TM 102630, Feb. 1991.

[3]Montgomery, R. C., Ghosh, D., and Kenny, S., "Analytic and Simulation Studies on the Use of Torque-Wheel Actuators for the Control of Flexible Robotic Arms," 1991 ASME Winter Annual Meeting, Atlanta, GA, Dec. 1991 (Paper B257).

[4]Yang, L.-F., Mikulas, M. M., Jr., Park, K. C., and Su, R., "Slewing Maneuvers and Vibration Control of Space Structures by Feedforward/Feedback Moment-Gyro Controls," *Journal of Dynamic Systems, Measurement and Control*, Vol. 117, No. 3, 1995, pp. 343–351.

[5]Aubrun, J. N., and Margulies, G., "Gyrodampers for Large Space Structures," NASA CR 159171, Feb. 1979.

[6]Greensite, A. L., *Analysis and Design of Space Vehicle Flight Control Systems (Control Theory*, Vol. 2), Spartan, New York, 1970.

[7]Li, Z., and Bainum, P. M., "Momentum Exchange: Feedback Control of Flexible Spacecraft Maneuvers and Vibration," *Journal of Guidance, Control, and Dynamics*, Vol. 15, No. 6, 1992, pp. 1354–1360.

[8]Kaplan, M. H., *Modern Spacecraft Dynamics and Control*, Wiley, New York, 1993.

[9]Tomizuka, M., Hu, J.-S., Chiu, T.-C., and Kamano, T., "Synchronization of Two Motion Control Axes Under Adaptive Feedforward Control," *Journal of Dynamic Systems, Measurement and Control*, Vol. 114, June 1992, pp. 196–203.

[10]Gill, P. E., Walter, M., and Margaret, H. W., *Practical Optimization*, Academic, New York, 1981.